Lab on a Chip

RSC Publishing

PAPER

View Article Online
View Journal | View Issue

Single-enzyme analysis in a droplet-based micro- and nanofluidic system†

Cite this: *Lab Chip*, 2013, **13**, 1955

Rerngchai Arayanarakool,[ab] Lingling Shui,[c] Servé W. M. Kengen,[d] Albert van den Berg[a] and Jan C. T. Eijkel*[a]

Received 1st October 2012,
Accepted 4th March 2013

DOI: 10.1039/c3lc41100a

www.rsc.org/loc

The kinetic activity of individual enzyme molecules was determined in aqueous droplets generated in a nano- and microfluidic device. To avoid high background noise, the enzyme and substrate solution was confined into femtoliter carriers, achieving high product concentrations from single-molecule encapsulation. The tiny droplets ($\phi \sim 2.5$–3 μm) generated from this fluidic system were highly monodisperse, beneficial for an analysis of single enzyme activity. The method presented here allows to follow large numbers of individual droplets over time. The instrumental requirements are furthermore modest, since the small droplet size allows to use of standard microscope and standard Pyrex glass chips as well as the use of relatively high enzyme concentrations (nM range) for single molecule encapsulation.

Introduction

Recently, many researchers have investigated the behavior of biomolecules on the single-molecular level to unravel phenomena which remain hidden in conventional bulk experiments.[1–3] Confinement of individual molecules can be obtained by means of attachment to a polymer-coated substrate,[1–3] but also with microfluidic technology. In this contribution we report on a study of single enzyme molecule activity using droplet-based micro-/nanofluidics. Single enzyme molecule activity has been investigated in microfluidic platforms using methods such as PDMS microwells,[4] surface-immobilized droplets[5] or liposomes, [6,7] but never in detail in droplets. Droplet-based microfluidics has many experimental advantages. It can be employed to generate scalable carriers to encapsulate individual molecules with high-throughput results.[8–11] In addition, microfluidic technology also enables precisely controlled manipulation of the generated carriers in an automated fashion.[11–15] The droplet-based platform is furthermore advantageous due to its flexibility to change the types of reactions and the amounts of reagents.[16,17] In addition, the droplet carriers can be made strongly monodisperse, simplifying the experimental analysis.[10,18] Single-enzyme analysis in droplet-based microfluidics has been demonstrated once before[19] but only in very large droplets ($\phi \sim 40$ μm) and for just one time point. Then the large droplets necessitated the use of highly-diluted enzyme solutions (110 fM) and a laser-based optical setup, while the femtoliter volume of the droplets generated from our device allows the use of a standard microscope and Pyrex glass chip as well as enzyme solutions at relatively high concentration (nM range). Furthermore, stable storage of the droplets allows us to observe the single enzyme kinetics in many individual droplets longitudinally in time.

Research on single enzymes can be performed by compartmentalizing the solution such, that single compartments contain single enzymes. One approach is to strongly dilute the enzyme and use large containers (Fig. 1B), another approach is to strongly decrease the compartment size (Fig. 1C). The latter approach has great advantages, since the product is much less diluted than in the large container. If for example a fluorescent product is formed, its observation will be much less hindered by the environmental background signal of solvent and device material. Smaller compartments thus allow higher concentrations of enzymes to be used and higher signal-to-noise ratios of the enzyme product molecules to be reached. The device material should furthermore have a low level of auto-fluorescence, making polymer-based materials generally much less suitable than glass. We therefore chose Borofloat type glass to fabricate our microfluidic device.[20,21] Moreover, our platform fabricated from a glass Borofloat material does not encounter the problem of the evaporation/dissolution of solvents and solutes into the chip material which is generally unavoidable in devices made from polymer-based materials such as polydimethyl-siloxane (PDMS).[22]

We use a micro-/nanochannel device to provide the femtoliter compartmented aqueous droplets for encapsulation

[a]*BIOS/Lab-on-chip group, MESA+ Institute for Nanotechnology, University of Twente, Enschede, P. O. Box 217, 7500 AE Enschede, The Netherlands.*
E-mail: j.c.t.eijkel@utwente.nl; Fax: 31+534893595; Tel: 31+534892691
[b]*Institute for Integrative Nanosciences, IFW Dresden, Helmholtzstrasse 20, Dresden 01069, Germany*
[c]*Institute of Electronic Paper Display, South China Normal University, Guangzhou, China*
[d]*Laboratory of Microbiology, Wageningen University, Wageningen, The Netherlands*
† Electronic supplementary information (ESI) available. See DOI: 10.1039/c3lc41100a

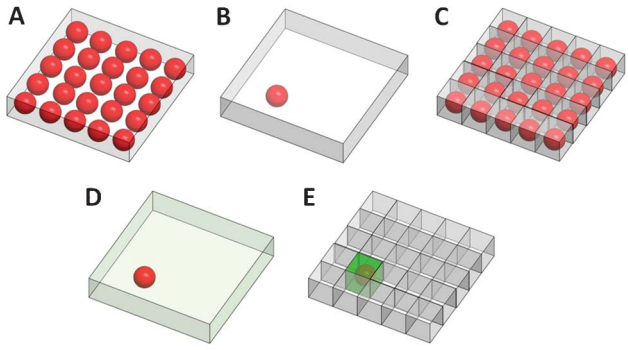

Fig. 1 (A) An illustration of the enzyme solution dissolved in an aqueous carrier (enzyme: red and water: grey). (B) By dilution, the single-molecule encapsulation can be achieved but the excess amount of solvent provides high background noise. (C) By compartmentalization, the enzyme solution is confined as tiny droplets containing single enzymes at high concentration. (D) When a single enzyme is enclosed in a large droplet, the fluorescent product gets much diluted, making optical detection more difficult. In addition to this, the background fluorescence from droplet and substrate is larger. (E) Smaller droplets increase the product concentration and decrease the background fluorescence. When the fluorescent product molecules are produced, the fluorescence intensity inside each droplet will gradually increase. The product formation rate in the droplet can then be used to determine the kinetic activity of this enzyme.

of single enzymes and the demonstration of their activity. A hyperthermophilic intrinsically stable enzyme (β-glucosidase) which produces a fluorescent product was chosen as model molecule. The histogram of the increasing fluorescence intensity in each droplet can then be used to determine the number of enzymes encapsulated in each compartment. In our system we can observe many droplets in parallel over a long period, so that, in case of single-molecule occupation, the evolution of the fluorescent product concentration in the individual droplets can be related to the temporal single enzyme kinetic activity.

Materials and methods

Glass-based micro- and nanofluidic device

The micro- and nanofluidic chip was made from a Borofloat glass substrate by standard etching techniques and subsequently hydrophobized by methods previously reported.[23] A schematic layout of the chip, containing a network of channels of 500 nm and 3 μm depth is shown in Fig. 2. To obtain the extremely low flow rates needed with standard syringe pumps, a flow-split channel design was used, as previously published.[24] The hydrophobized chip was mounted into the in-house built chip holder and placed onto an inverted fluorescence microscope (DMI 5000 M, Leica) equipped with mercury lamp and high-sensitivity camera (EMCCD, Andor Ixon, UK). The solutions were loaded into the chip by using a flow-driven neMESYS pump. (See Fig. S1 in Electronic Supporting Information; ESI†)

Fluidic connections

The glass-based chip was mounted into an in-house manufactured chip holder and connected to a neMESYS syringe pump (Cetoni, Korbussen, Germany) with fused silica tubing (ϕ = 360 μm), and fluidic connectors bought from Upchurch Scientific (WA, USA). The neMESYS syringe pump is a flow rate-driven pump with three modules enabling to individually manipulate the flow rate of three different solutions into the fluidic chip.

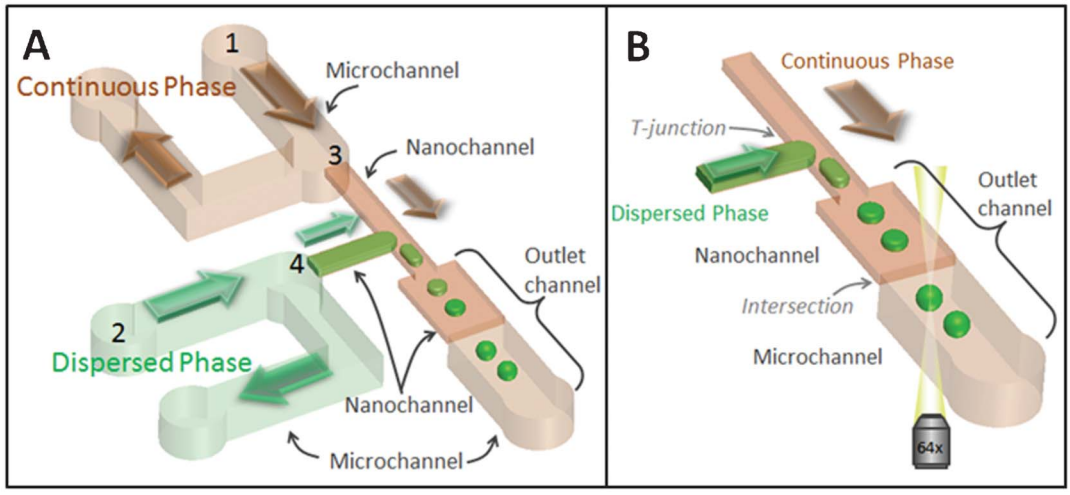

Fig. 2 (A) Schematic of the droplet generator using a micro- and nanofluidic network. A continuous phase (silicone oil; shown in orange) and a dispersed phase (enzyme and substrate solution; shown in green) and a were separately loaded into the microchannels at position 1 and 2, respectively. Minute amounts of continuous and dispersed phases split off into the nanochannels sections at the split junctions at position 3 and 4, respectively. A zoom-in view of the nanofluidic network as well as the outlet microchannel is shown in (B). At the T-junction, femtoliter droplets split off from the aqueous solution and flowed to the outlet nanochannel. Finally, at the intersection between nano- and microchannels, the squeezed droplets obtained a spherical shape and entered the outlet microchannel where the time-resolved fluorescent measurement was performed. The arrows express the direction of the fluid flows. The depths of the microchannel and nanochannels are 3 and 0.5 μm, respectively.

Optical setup

The chip holder incorporating a fluidic chip was placed on top of an epifluorescence microscope (DMI 5000 M, Leica) equipped with a specific filter cube (L5) for the excitation and emission wavelengths of 480 and 520 nm, respectively and a mercury lamp for illumination. An electron multiplying CCD camera (EMCCD, Andor Ixon, UK) was used for light collection.[27] The fluid flow and emulsion were visualized and recorded by the Andor Solis program.

Enzyme kinetics

The enzymatic reaction of β-glucosidase was studied by using fluorescein-β-D-glucopyranoside (FDGlu) as a substrate, yielding fluorescein as product. The increase in fluorescence intensity was used to determine the kinetic activity. In short, since the enzyme obeys Michaelis–Menten kinetics and the substrate concentration is much higher than the Michaelis–Menten constant, we observe the maximal production rate of the enzyme for which holds $V_{max} = K_{cat}[E]$ where K_{cat} is the turnover number and [E] the enzyme concentration (number of enzymes/droplet) [for further details please see the supporting information]. To interpret the droplet fluorescence intensity in terms of fluorescein concentration, a calibration curve was made using known fluorescein concentrations (see section 2 and Fig. S2 in ESI†).

Enzyme, chemicals and solutions

Droplets were produced from a dispersed phase containing β-glucosidase (0.1 nM), FDGlu (200 μM) in PBS solution (pH 7) and a continuous oil phase (silicone oil with 4% Span80), which were individually injected into the fluidic system. In the experiment in the presence of an anti-oxidant reagent, n-propyl gallate (5% w/v) was added to the aqueous solution before injection into the fluidic device. The β-glucosidase used in this study is originally derived from the hyperthermophilic archaeon *Pyrococcus furiosus*[25] It exhibits an intrinsic high stability with a half-life of 85 h at 100 °C. Despite its high temperature optimum of 103 °C, it still shows activity at moderate temperatures. The enzyme preparation used here is obtained through heterologous expression of the *celB* gene in *E.coli* and subsequent purification of the protein as reported previously.[25,26] The enzyme was provided by the Laboratory of Microbiology, Wageningen University, The Netherlands. FDGlu was purchased from Invitrogen. The other chemicals were purchased from Sigma-Aldrich, The Netherlands. Before mixing, each solution was degassed by placing into a desiccator to remove oxygen molecules in the solution.

Enzyme activity in bulk experiment

To verify the reliability of the experiment performed in our droplet-based microfluidic platform, we compared the kinetic activity obtained from our device to that from a bulk experiment using a fluorescence spectrophotometer (Perkin Elmer).

Protocol to determine enzyme activity in droplets

The aqueous and oil solutions were separately loaded into the fluidic device to create droplets. After a large amount of generated droplets had entered the outlet channel (see Fig. 2), all syringe pumps were stopped to halt the movement of droplets. To follow the evolution of the fluorescence intensity in each droplet, at regular intervals snapshots of the array of droplets were made by the EMCCD camera. For each snapshot the fluorescence illumination was just 5 s to limit product photobleaching. The fluorescence intensities in each individual droplet were later determined by using a program ImageJ (NIH Image). The array also contained some (2–10%) larger (merged) droplets, but only the data from non-merged droplets in the diameter range of 2.5–3 μm were used for the analysis in this experiment. All experiments were performed at room temperature (25 °C).

Results and discussion

Droplet generation

For the purpose of single-enzyme encapsulation a fluidic platform consisting of a microfluidic network and a T-junction nanofluidic network was used (Fig. 2). The oil solution and the aqueous solution were individually loaded into the device at positions 1 and 2 indicated in Fig. 2 Left, respectively, flowing through the microchannels as indicated by the large arrows in Fig. 2 Left. When reaching the flow split at the positions 3 and 4 for the oil and aqueous phase networks, respectively, tiny portions of both fluids were split off into the nanochannels as indicated as the small arrows. Subsequently at the T-junction in the nanofluidic network (Fig. 2 Right), shear was exerted on the tip of the dispersed phase stream by the continuous phase generating femtoliter water droplets which flowed to the outlet nanochannel.

After formation the droplets were squeezed by the top and bottom walls of the nanochannel, generating a non-spherical shape. The squeezed droplets in the nanochannels in principle would provide a larger detection area as compared to spherical droplets of the same volume, but the squeezed droplets were found to be prone to merging. When a downstream outlet microchannel was added to our fluidic network (Fig. 2), in it the squeezed droplets relaxed to a spherical shape driven by a reduction of the interfacial energy. The spherical droplets proved more stable to merging and were therefore preferably used as carriers for prolonged observation. In the experiments with nPG the diameter of around 90% of the droplets was found to range from 2.5–3.1 μm (average 2.9 μm) in diameter. The remainder of the droplets had a larger diameter with peaks at approximately 3.3, 4.0 and 4.6 μm (Fig. S8 in ESI†), probably resulting from merger of 2, 3, 4 droplets during the prolonged measurement. Only the data of the droplets in the range of 2–5–3.1 μm was used for analysis. In the experiments without nPG approximately 97% droplets was found to have a diameter around 2.9 μm, indicating much less droplet fusion.

Photobleaching

One drawback of the fluorescein molecule is its relatively high rate of photobleaching, especially in the presence of oxygen molecules.[28] Since this would lead to the misinterpretation of the amount of fluorescent molecules in the system, the solution was only exposed to the excitation wavelength for a

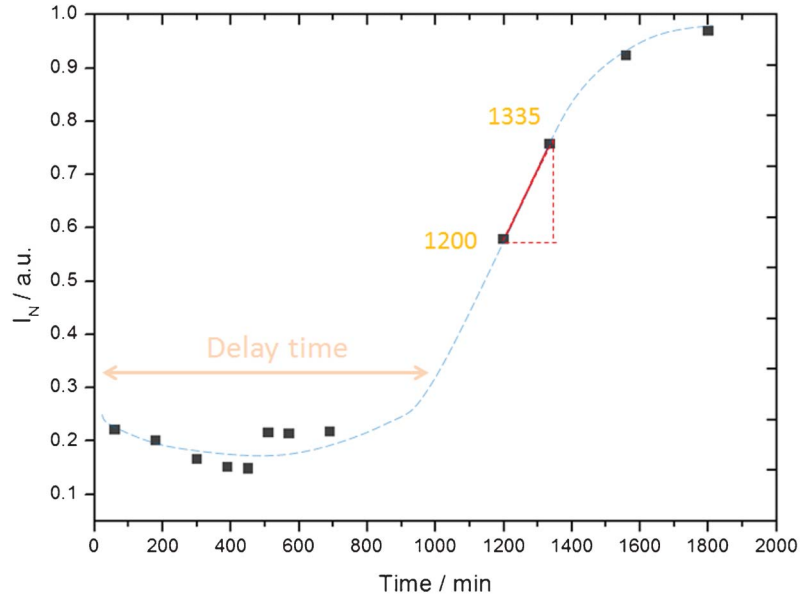

Fig. 3 The evolution of the fluorescence intensity from the enzymatic reaction in the presence of nPG. In the first part, labeled as 'delay time', the signal from the fluorescein remains lower than the background fluorescence. In the second part, the fluorescence intensity increases above the background fluorescence level and is used to determine the enzyme kinetics. The continuous phase was silicone oil with 4% Span80 and the aqueous phase was FDGlu (200 μM), β-glucosidase (0.1 nM), and nPG (5% w/v) in PBS solution.

few seconds for every single snapshot taken. Furthermore, oxygen molecules were removed from the system. Initially we also added the anti-oxidant n-propyl gallate (nPG) to the solution.[29–31] The experimental details of the effect on photobleaching in our system are described in section 3 of the ESI†.

Enzyme activity in bulk experiment

From the experiment on the fluorescence spectrophotometer, the obtained product formation rates of the reaction are plotted as a function of the substrate concentration (Fig. S7 in ESI†). The data points were fitted using the Michaelis–Menten equation, resulting in K_m (Michalis–Menten constant) and K_{cat} (turnover number) values of 25.6 μM and 5.7 s^{-1}, respectively.

Enzymatic reaction in the presence of n-propyl gallate

After droplet formation, the fluorescence intensity of single droplets was plotted against time (Fig. 3). Initially a fluctuating background signal was measured, implying that the fluorescence from the fluorescent product in this time remained smaller than the background signal. This time during which no product was detectable is labeled as "*delay time*". After this delay time, the fluorescence intensity for some period increased proportional with time. The rate of increase of fluorescence intensity in this period was taken to represent the

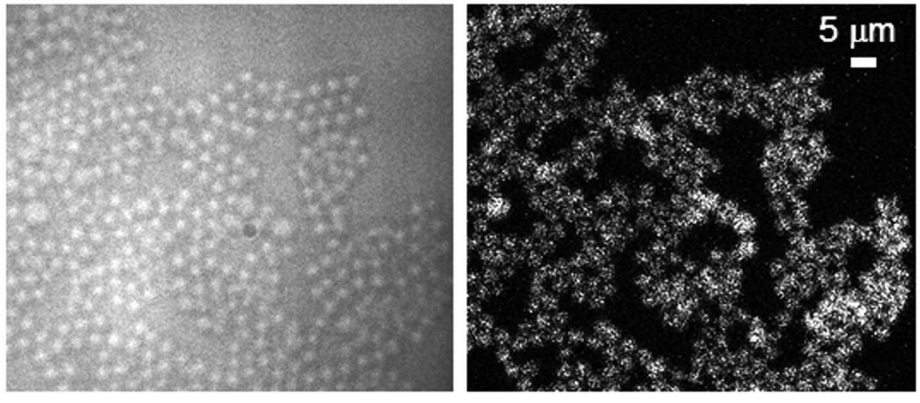

Fig. 4 Encapsulation of enzyme and substrate into droplets. (Left) Bright-field image of the array of droplets; (Right) Fluorescence image of the same system after incubation for 1335 min. A few merged droplets are visible, which were excluded from analysis. The droplet size of the non-merged droplets is around 2.9 μm. The continuous phase was silicone oil with 4% Span80 and the aqueous phase was FDGlu (200 μM), β-glucosidase (0.1 nM), and nPG (5% w/v) in PBS solution.

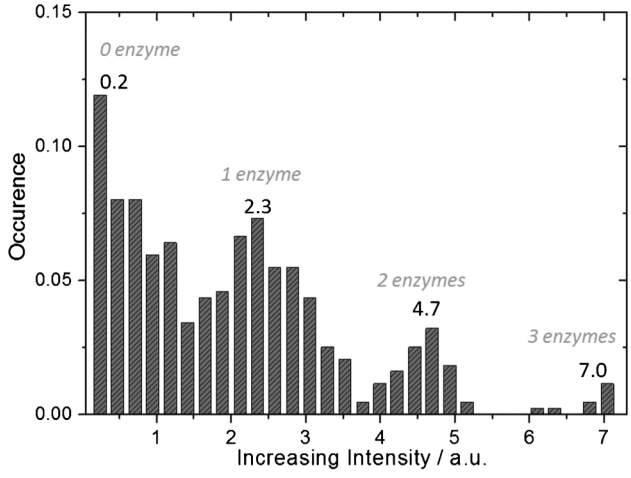

Fig. 5 Histogram of the increasing fluorescence intensity from the 1200th to the 1335th minute. Four peaks can be interpreted as indicating the occupancy of droplets by (0, 1, 2 and 3) enzymes. The continuous phase was silicone oil with 4% Span80 and the aqueous phase was FDGlu (200 μM), β-glucosidase (0.1 nM), and nPG (5% w/v) in PBS solution.

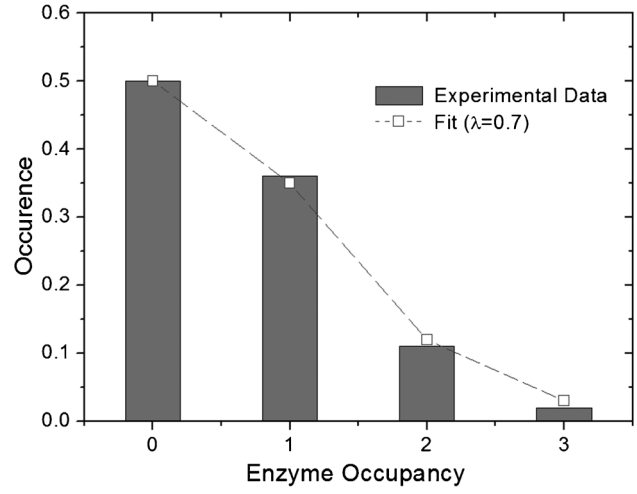

Fig. 6 Distribution of the occupancy of enzyme in each droplet (bar chart) fitted to a Poisson distribution with a mean occupancy $\lambda = 0.7$ (dash line). The continuous phase was silicone oil with 4% Span80 and the aqueous phase was FDGlu (200 μM), β-glucosidase (0.1 nM), and nPG (5% w/v) in PBS solution.

kinetic activity of the enzyme. Specifically, the fluorescence intensity change between the 1200th and the 1335th minute was used to extract the kinetic activity. Images of the array of droplets containing the enzyme and substrate solution in bright field and fluorescence imaging are shown in Fig. 4.

The increase in fluorescence intensity in each droplet between minutes 1200 and 1335 is plotted in a histogram (Fig. 5) revealing that it is periodically enhanced and can be categorized into four peaks (0.2, 2.3, 4.7 and 7.0). According to Michaelis–Menten kinetics, the enzyme activity is given by $V_{max} = K_{cat}[E]$ (see ESI†). We interpreted these peaks as generated by 0, 1, 2 or 3 enzyme molecules encapsulated in the droplets since the intensity increase of the third (2 molecules) and fourth peak (three molecules) is approximately two and three times higher than the second peak (1 molecule), respectively. The resulting turnover number K_{cat} for the enzyme activity is around 1.6 molecules of product per second.

The histogram of the occupancy of this enzyme fits well to a Poisson distribution (Fig. 6) which is expressed by $f(\lambda,x) = \frac{\lambda^x e^{-\lambda}}{x!}$ where λ is a mean number of enzymes per droplet and x is the number of enzymes per droplet. In this experiment a mean occupancy λ of 0.7 molecules/droplet was measured while the calculated occupancy for droplets with a diameter of 3 μm and an enzyme concentration of 0.1 nM is approximately 0.9 molecules/droplet. These data strongly suggest a successful encapsulation of single enzymes into the droplets.

In these experimental results, a K_{cat} was obtained ($1.6\ s^{-1}$) which is significantly lower than in the bulk experiment ($5.7\ s^{-1}$). We hypothesized that this lower kinetic activity could result from inhibitory activity of n-propyl gallate (nPG) added as an anti-oxidant reagent, (see also the discussion below). Therefore the further experiments were performed without the addition of nPG.

Enzymatic reaction in the absence of n-propyl gallate

In this experiment, the aqueous solution containing the β-glucosidase (0.1 nM) and the substrate solution (200 μM) was prepared in PBS buffer solution without the addition of nPG. The droplet emulsion was subsequently prepared with the same procedure as mentioned above. The evolution of the fluorescence intensity recorded in a single droplet in the absence of nPG is illustrated in Fig. 7. A much shorter delay time (240 min *vs.* 1000 min) was observed as compared to the previous experiment in the presence of nPG (Fig. 3).

The increase in the fluorescence intensity and hence the enhancement of fluorescent product in each droplet from the 240th to the 260th minute is plotted in a histogram (Fig. 8) for an enzyme concentration of 0.1 nM. From this histogram (Fig. 8), the concentration of fluorescein was seen to be periodically increased in four peaks which can again be interpreted as corresponding to different numbers of enzymes encapsulated into the droplets. The obtained K_{cat} from these experiments was around $3.8\ s^{-1}$.

To confirm this single-enzyme encapsulation and our interpretation, another experiment was performed by using a two-fold higher concentration of the enzyme (0.2 nM). The histogram of the increasing concentration of fluorescein in each droplet is plotted in Fig. 9. For this case the resulting K_{cat} was around $4.5\ s^{-1}$.

In Fig. 10, the experimental data obtained from the enzyme solutions are plotted as fractional occurrence of droplets with enzyme occupancy (0, 1, 2 or 3) using bars of dark grey and light grey for the 0.1 and 0.2 nM of enzyme solution, respectively. The Poisson distributions for the first and second cases are depicted as dotted and straight lines, respectively. As shown, the histograms for both experiments can be well fitted to Poisson distributions (Fig. 10) with mean occupancies λ of 0.62 and 1.24. The average enzyme occupancy in one droplet (diameter of 2.9 μm) by calculation is 0.7 and 1.4 molecules for

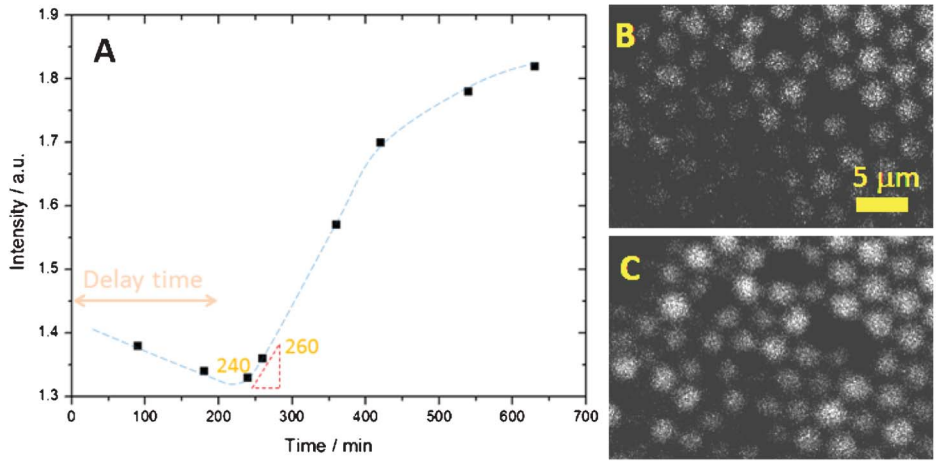

Fig. 7 The evolution of the fluorescence intensity from the enzymatic reaction in the absence of nPG. The data at the 240th and 260th minute were used to estimate the enzyme kinetics. The snapshots of the array of droplets containing enzyme and substrate molecules without the addition of nPG at minute 240 (B), and 260 (C) are shown.

the enzyme concentrations of 0.1 and 0.2 nM, respectively, corresponding well to the mean occupancies (λ) from the fitted Poisson curves.

These data strongly indicate that single-enzyme encapsulation was obtained into the femtoliter aqueous droplets generated in our device. The evolution of the fluorescence intensity as determined from the kinetic activity of the encapsulated enzymes (3.8–4.5 s^{-1}) was slightly lower than the enzymatic kinetic activity observed in bulk experiments (5.7 s^{-1}), but much higher than the kinetic activities observed in the presence of nPG (see discussion in the following section).

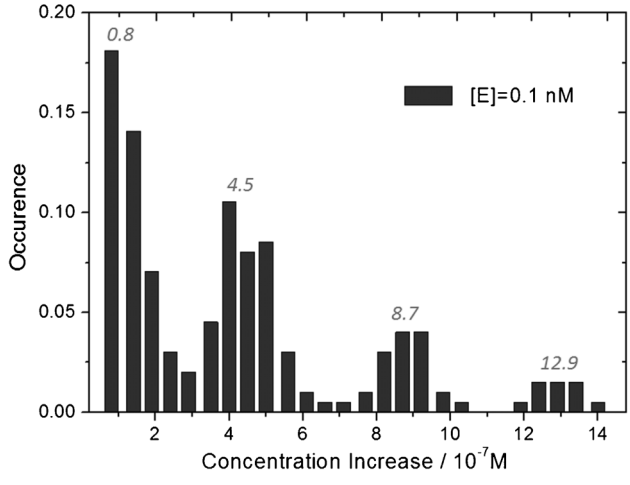

Fig. 8 The increasing fluorescence intensity from the 240th to the 260th minute. Four peaks can be interpreted as indicating the occupancy of droplets by (0, 1, 2 and 3) enzymes. The continuous phase was silicone oil with 4% Span80 and the aqueous phase was FDGlu (200 μM) and β-glucosidase (0.1 nM) in PBS solution.

Discussion

In the droplet experiments without nPG we obtained a kinetic activity about 25% lower than in the bulk experiment. This observation corresponds to several literature reports mentioning that the kinetic activity obtained in droplets in microfluidic devices was lower than in the bulk experiments.[32,33] In literature possible explanations for this phenomenon are under discussion.

As already mentioned, we also observed a *delay time* before an approximately linear increase of fluorescent intensity was observed (Fig. 3 and Fig. 7). Given the lowest detectable concentration of fluorescein as 7000 molecules/droplet (as separately determined using a calibration curve), and given a K_{cat} of 3.8 s^{-1}, the fluorescence intensity should start to increase around the 30th minute. In our experiment however, it took place only at around the 230th minute (Fig. 7). Therefore the main cause of the delay cannot be the background fluorescence. A possible explanation is that the fluorescent product initially is consumed by a process which becomes saturated during the delay time. What could this process be? Possibly a temporary adsorption of the enzyme could occur at the water/oil interface. However, it would be hard to explain why the enzyme would adsorb to the interface only initially. A more probable explanation is therefore that the fluorescence of the product initially is suppressed. This can happen if the generated fluorescent product is adsorbed at the water/oil interface, resulting in suppressed fluorescence. After saturation of the interface ("*delay time*"), an increasing fluorescence intensity will then be observed. It is also possible that the fluorescein molecules diffuse into the oil phase in an uncharged (hence non-fluorescent) state. This process has indeed recently been observed in droplets with fluorescein and has also been modeled.[34–37] Only after equilibrium is reached between droplets and oil, the fluorescein molecules produced from the enzymatic reaction will then remain inside the

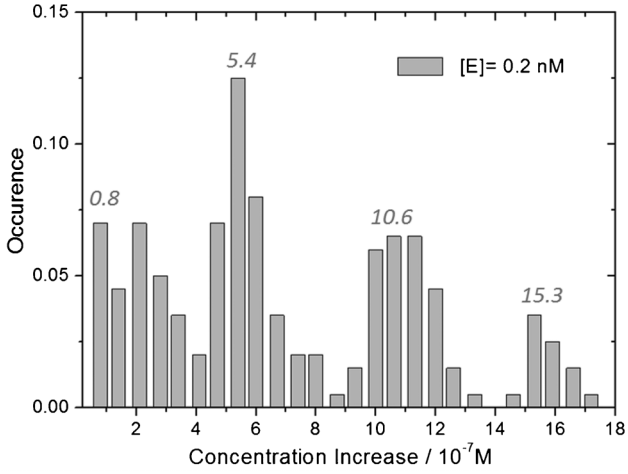

Fig. 9 The increasing fluorescence intensity from the 20th to the 30th minute. Four peaks can be interpreted as indicating the occupancy of droplets by (0, 1, 2 and 3) enzymes. The continuous phase was a silicone oil with 4% Span80 and the aqueous phase was FDGlu (200 μM) and β-glucosidase (0.2 nM) in PBS solution.

droplet resulting in an increasing fluorescence intensity. At present we cannot distinguish between both hypotheses, though on the basis of recent literature reports the latter seems more probable.

In the experiment in the presence of n-propyl gallate (nPG), the measured kinetic activity was only 1.6 s^{-1}, while it increased to 3.8–4.5 s^{-1} in its absence. On the basis of this we hypothesize that the nPG behaves as an inhibitor for the enzymatic reaction. When considering the structure of nPG as shown in Fig. 11A, its structure is somewhat similar to one side of the structure of cellobiose which is a natural substrate

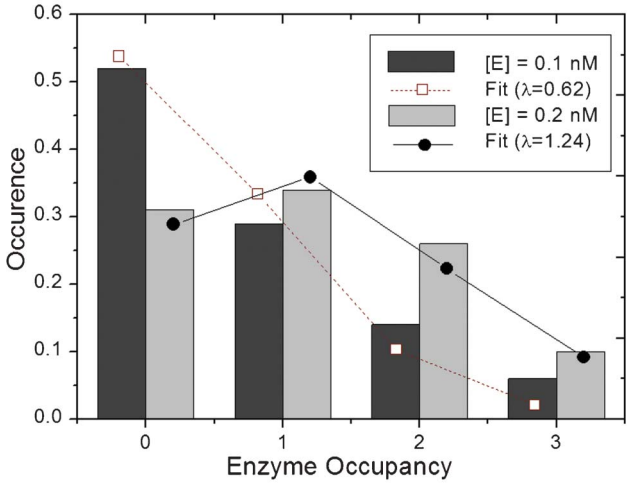

Fig. 10 Two histograms express the distribution of the occupancy of enzymes (0, 1, 2 and 3) per droplet. The dark grey bar and the light grey bar depict the data distribution when the enzyme solution was 0.1 and 0.2 nM, respectively. The data for 0.1 and 0.2 nM enzyme solution were fitted to a Poisson distribution as shown by a dotted line and a solid line, respectively. The mean occupancy λ used for these fits was 0.62 and 1.24, respectively.

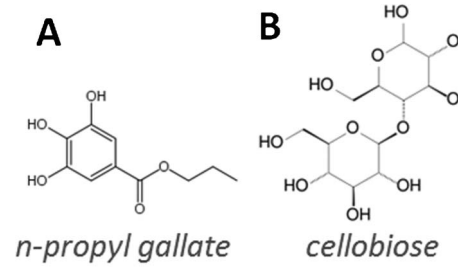

Fig. 11 Molecular structures of (A) n-propyl gallate and (B) cellobiose, a natural substrate for β-glucosidase.

of β-glucosidase (see Fig. 11). Thus, nPG might indeed be a (partial) inhibitor of the glucosidase enzyme.

Finally, in the experiment in the absence of n-propyl gallate (nPG), the fluorescein molecules produced from the enzymatic reaction might undergo photobleaching, which might be a general cause of the slightly lower values for the activity obtained in comparison to the bulk experiment. The half time of the fluorescein molecule under illumination from our setup is around 5 min (see Fig. S4 in ESI†). For the observations, the UV light was, however, illuminated for a few seconds only for every single snapshot taken, resulting in a cumulative exposure time of approximately 30 s, implying a negligible photobleaching effect.

Conclusion

We have demonstrated a micro- and nanofluidic platform for creating droplet arrays encapsulating single enzyme molecules. The enzyme -glucosidase, generating fluorescent product, was selected for a first demonstration. Femtoliter aqueous droplets were generated in a hydrophobized glass-based device. The histogram of the rate of fluorescence intensity increase and hence the turnover number of the enzymatic reaction in each droplet showed periodically-increased peaks revealing the occupancy of droplets by multiples of a single enzyme. The distributions fitted well to a Poisson distribution verifying the achieved encapsulation of single enzymes. The kinetic activity observed was somewhat lower than that obtained from a bulk experiment.

References

1 H. P. Lu, L. Y. Xun and X. S. Xie, *Science*, 1998, **282**, 1877–1882.
2 W. Min, I. V. Gopich, B. P. English, S. C. Kou, X. S. Xie and A. Szabo, *J. Phys. Chem. B*, 2006, **110**, 20093–20097.
3 K. Velonia, O. Flomenbom, D. Loos, S. Masuo, M. Cotlet, Y. Engelborghs, J. Hofkens, A. E. Rowan, J. Klafter, R. J. M. Nolte and F. C. de Schryver, *Angew. Chem., Int. Ed.*, 2005, **44**, 560–564.

4 Y. Rondelez, G. Tresset, K. V. Tabata, H. Arata, H. Fujita, S. Takeuchi and H. Noji, *Nat. Biotechnol.*, 2005, **23**, 361–365.
5 S. Sakakihara, S. Araki, R. Iino and H. Noji, *Lab Chip*, 2010, **10**, 3355–3362.
6 T. M. Hsin and E. S. Yeung, *Angew. Chem., Int. Ed.*, 2007, **46**, 8032–8035.
7 S. M. Christensen, P. Y. Bolinger, N. S. Hatzakis, M. W. Mortensen and D. Stamou, *Nat. Nanotechnol.*, 2012, **7**, 51–55.
8 E. Brouzes, M. Medkova, N. Savenelli, D. Marran, M. Twardowski, J. B. Hutchison, J. M. Rothberg, D. R. Link, N. Perrimon and M. L. Samuels, *Proc. Natl. Acad. Sci. U. S. A.*, 2009, **106**, 14195–14200.
9 P. Garstecki, M. J. Fuerstman, H. A. Stone and G. M. Whitesides, *Lab Chip*, 2006, **6**, 437–446.
10 A. J. C. Kuehne and D. A. Weitz, *Chem. Commun.*, 2011, **47**, 12379–12381.
11 L. Mazutis, A. F. Araghi, O. J. Miller, J. C. Baret, L. Frenz, A. Janoshazi, V. Taly, B. J. Miller, J. B. Hutchison, D. Link, A. D. Griffiths and M. Ryckelynck, *Anal. Chem.*, 2009, **81**, 4813–4821.
12 P. Abbyad, R. Dangla, A. Alexandrou and C. N. Baroud, *Lab Chip*, 2011, **11**, 813–821.
13 B. Lee and J. Y. Yoo, *Microfluid. Nanofluid.*, 2011, **11**, 685–693.
14 L. Mazutis, J. C. Baret and A. D. Griffiths, *Lab Chip*, 2009, **9**, 2665–2672.
15 W. H. Tan and S. Takeuchi, *Lab Chip*, 2006, **6**, 757–763.
16 T. T. Fu, D. Funfschilling, Y. Ma and H. Z. Li, *Microfluid. Nanofluid.*, 2010, **8**, 467–475.
17 S. J. Zeng, B. W. Li, X. O. Su, J. H. Qin and B. C. Lin, *Lab Chip*, 2009, **9**, 1340–1343.
18 L. L. Shui, A. van den Berg and J. C. T. Eijkel, *Microfluid. Nanofluid.*, 2011, **11**, 87–92.
19 H. N. Joensson, M. L. Samuels, E. R. Brouzes, M. Medkova, M. Uhlen, D. R. Link and H. Andersson-Svahn, *Angew. Chem., Int. Ed.*, 2009, **48**, 2518–2521.
20 B. Lu, S. Y. Zheng, B. Q. Quach and Y. C. Tai, *Lab Chip*, 2010, **10**, 1826–1834.
21 A. Piruska, I. Nikcevic, S. H. Lee, C. Ahn, W. R. Heineman, P. A. Limbach and C. J. Seliskar, *Lab Chip*, 2005, **5**, 1348–1354.
22 Y. S. Heo, L. M. Cabrera, J. W. Song, N. Futai, Y. C. Tung, G. D. Smith and S. Takayama, *Anal. Chem.*, 2007, **79**, 1126–1134.
23 R. Arayanarakool, L. L. Shui, A. van den Berg and J. C. T. Eijkel, *Lab Chip*, 2011, **11**, 4260–4266.
24 L. L. Shui, E. S. Kooij, D. Wijnperle, A. van den Berg and J. C. T. Eijkel, *Soft Matter*, 2009, **5**, 2708–2712.
25 S. W. M. Kengen, E. J. Luesink, A. J. M. Stams and A. J. B. Zehnder, *Eur. J. Biochem.*, 1993, **213**, 305–312.
26 J. H. G. Lebbink, T. Kaper, S. W. M. Kengen, J. van der Oost and W. M. de Vos, *Methods Enzymol.*, 2001, **330**, 364–379.
27 O. Castillo-Fernandez, G. B. Salieb-Beugelaar, J. W. van Nieuwkasteele, J. G. Bomer, M. Arundell, J. Samitier, A. van den Berg and J. C. T. Eijkel, *Electrophoresis*, 2011, **32**, 2402–2409.
28 L. L. Song, E. J. Hennink, I. T. Young and H. J. Tanke, *Biophys. J.*, 1995, **68**, 2588–2600.
29 H. Giloh and J. W. Sedat, *Science*, 1982, **217**, 1252–1255.
30 A. K. Gaigalas, L. Wang, K. D. Cole and E. Humphries, *J. Phys. Chem. A*, 2004, **108**, 4378–4384.
31 M. Battaglia, D. Pozzi, S. Grimaldi and T. Parasassi, *Biotech. Histochem.*, 1994, **69**, 152–156.
32 Y. Liu, S. Y. Jung and C. P. Collier, *Anal. Chem.*, 2009, **81**, 4922–4928.
33 L. Mazutis, J. C. Baret, P. Treacy, Y. Skhiri, A. F. Araghi, M. Ryckelynck, V. Taly and A. D. Griffiths, *Lab Chip*, 2009, **9**, 2902–2908.
34 Y. H. Chen, A. W. Gani and S. K. Y. Tang, *Lab Chip*, 2012, **12**, 5093–5103.
35 N. Wu, F. Courtois, Y. G. Zhu, J. Oakeshott, C. Easton and C. Abell, *Electrophoresis*, 2010, **31**, 3121–3128.
36 P. R. Marcoux, M. Dupoy, R. Mathey, A. Novelli-Rousseau, V. Heran, S. Morales, F. Rivera, P. L. Joly, J. P. Moy and F. Mallard, *Colloids Surf., A*, 2011, **377**, 54–62.
37 F. Courtois, L. F. Olguin, G. Whyte, A. B. Theberge, W. T. S. Huck, F. Hollfelder and C. Abell, *Anal. Chem.*, 2009, **81**, 3008–3016.

